BIOCHEMISTRY

 Volume 44, Number 23 June 14, 2005

Articles

Crystal Structure of *Escherichia coli* Penicillin-Binding Protein 5 Bound to a Tripeptide Boronic Acid Inhibitor: A Role for Ser-110 in Deacylation†

George Nicola,‡ Sridhar Peddi,§ Miglena Stefanova,§ Robert A. Nicholas,*,|| William G. Gutheil,*,§ and Christopher Davies*,‡

Department of Biochemistry, Medical University of South Carolina, Charleston, South Carolina 29425, Division of Pharmaceutical Sciences, University of Missouri—Kansas City, 5005 Rockhill Road, Kansas City, Missouri 64110, and Department of Pharmacology, CB 7365 Jones, University of North Carolina at Chapel Hill, Chapel Hill, North Carolina 27599-7365

Received December 22, 2004; Revised Manuscript Received April 8, 2005

ABSTRACT: Penicillin-binding protein 5 (PBP 5) from *Escherichia coli* is a well-characterized D-alanine carboxypeptidase that serves as a prototypical enzyme to elucidate the structure, function, and catalytic mechanism of PBPs. A comprehensive understanding of the catalytic mechanism underlying D-alanine carboxypeptidation and antibiotic binding has proven elusive. In this study, we report the crystal structure at 1.6 Å resolution of PBP 5 in complex with a substrate-like peptide boronic acid, which was designed to resemble the transition-state intermediate during the deacylation step of the enzyme-catalyzed reaction with peptide substrates. In the structure of the complex, the boron atom is covalently attached to Ser-44, which in turn is within hydrogen-bonding distance to Lys-47. This arrangement further supports the assignment of Lys-47 as the general base that activates Ser-44 during acylation. One of the two hydroxyls in the boronyl center (O2) is held by the oxyanion hole comprising the amides of Ser-44 and His-216, while the other hydroxyl (O3), which is analogous to the nucleophilic water for hydrolysis of the acyl—enzyme intermediate, is solvated by a water molecule that bridges to Ser-110. Lys-47 is not well-positioned to act as the catalytic base in the deacylation reaction. Instead, these data suggest a mechanism of catalysis for deacylation that uses a hydrogen-bonding network, involving Lys-213, Ser-110, and a bridging water molecule, to polarize the hydrolytic water molecule.

Penicillin-binding proteins (PBPs),[1] which are the lethal targets of β-lactam antibiotics, are ubiquitous bacterial enzymes that catalyze the final steps in cell-wall biosynthesis (reviewed in refs *1*−*3*). The bacterial cell wall is composed of glycan strands consisting of a repeating disaccharide, *N*-acetylglucosamine-β-1,4-*N*-acetylmuramic acid, in which the *N*-acetylmuramic acid residues are substituted with a pentapeptide chain. The structure of the peptide moiety varies among different bacteria, but in *Escherichia coli*, the peptide

† This work was supported by the National Institutes of Health Grants GM66861 (to C.D.), AI36901 (to R.A.N.), and GM60149 (to W.G.G.).

* To whom correspondence should be addressed: Department of Biochemistry, Medical University of South Carolina, Charleston, SC 29425. Telephone: (843) 792-1468. Fax: (843) 792-8568. E-mail: davies@musc.edu (C.D.); Division of Pharmaceutical Sciences, University of Missouri—Kansas City, 5005 Rockhill Road, Kansas City, MO 64110. Telephone: (816) 235-2424. Fax: (816) 235-5190. E-mail: gutheilw@umkc.edu (W.G.G.); and Department of Pharmacology, University of North Carolina, Chapel Hill, NC 27599. Telephone: (919)966-6547. Fax: (919)966-5640. E-mail: nicholas@med.unc.edu (R.A.N.).

‡ Medical University of South Carolina.

§ University of Missouri—Kansas City.

|| University of North Carolina at Chapel Hill.

[1] Abbreviations: Boc, butyloxycarbonyl; Cbz, benzyloxycarbonyl; CPase, carboxypeptidase; DCM, dichloromethane; DIPEA, diisopropylethylamine; DMAP, (dimethylamino)pyridine; DMF, dimethylformamide; Fm, fluorenylmethyl; HMM, high molecular mass; HPLC, high-pressure liquid chromatography; IBCF, isobutylchloroformate; LC/MS, liquid chromatography/mass spectrometry; LMM, low molecular mass; *m*-DAP, *meso*-diaminopimelic acid; NMM, *N*-methylmorpholine; PBP, penicillin-binding protein; THF, tetrahydrofuran.

10.1021/bi0473004 CCC: $30.25
Published on Web 05/19/2005

Scheme 1

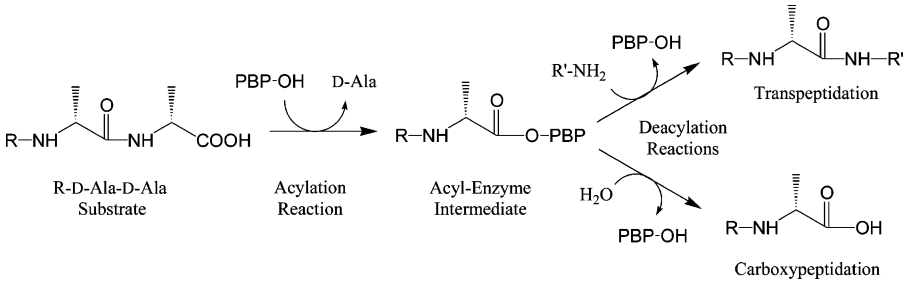

chain is L-Ala-γ-D-Glu-*m*-DAP-D-Ala-D-Ala (*m*-DAP = *meso*-diaminopimelic acid). The invariant properties of the peptide chain include a free amino group in the side chain of the third residue (i.e., *m*-DAP) and D-Ala-D-Ala at the C terminus. The cross-linking of the peptide chains from adjacent glycan strands, which is catalyzed by PBPs, confers rigidity to the cell wall and is critical for cell viability.

Bacteria have multiple PBPs (*4*), and these can be grouped into two classes: the high molecular mass (HMM) PBPs, which are essential for cell viability and catalyze transpeptidation and sometimes transglycosylation of disaccharide−pentapeptide chains during peptidoglycan synthesis, and low molecular mass (LMM) PBPs, which are not essential for cell viability and catalyze carboxypeptidase (CPase), transpeptidase, and/or endopeptidase reactions (reviewed in ref *5*). PBPs catalyze a two-step reaction: acylation, in which an active-site serine nucleophile on the PBP attacks the penultimate D-Ala residue to form an acyl−enzyme complex with the peptide chain, releasing the C-terminal D-Ala, and deacylation, which varies depending on the PBP (Scheme 1). For HMM PBPs, deacylation occurs when an amino group on a second peptide substrate acts as an acceptor, resulting in a peptide cross-link between two adjacent peptidoglycan strands (transpeptidation). However, in most LMM PBPs, the acceptor is a water molecule and the outcome is hydrolysis (carboxypeptidation). β-Lactam antibiotics, by virtue of their structural similarity to the acyl-D-Ala-D-Ala portion of the peptide chain (*6*), inhibit PBPs by forming long-lived serine acyl−enzyme complexes, preventing the enzymes from performing their normal enzymatic functions.

Although not essential for cell viability, several LMM PBPs have been found to play important roles in cell division and cell shape, including PBP 3 from *Streptococcus pneumoniae* (*7*), PBP 5 from *E. coli* (*8*), and PBPs 3 and 4 from *Neiserria gonorrhoeae* (*9*). The similarity between all PBPs in terms of active-site sequence (*2*) and architecture (*10*−*14*) makes LMM PBPs excellent models to elucidate the enzymological and mechanistic properties of the PBP class of enzymes as a whole. One of the best-studied LMM PBPs is PBP 5 from *E. coli*. This enzyme catalyzes both D-alanine CPase and weak transpeptidase activities typical of LMM PBPs (*15*) and is important for normal cell shape in *E. coli* in certain genetic backgrounds (*8*, *16*, *17*).

The crystal structures of soluble constructs of both wild-type PBP 5 (*18*) and a deacylation-defective mutant (PBP 5′) (*12*) have provided clues regarding the catalytic mechanism of the enzyme and suggest that, by abstracting a proton from the γ hydroxyl of Ser-44, Lys-47 is the general base for acylation (*12*, *15*). In contrast, the mechanism of deacylation remains unclear, but one possibility is that Lys-47 also acts as a general base in deacylation by abstracting a proton from an attacking water molecule during hydrolysis (*15*).

A logical step toward understanding the catalytic mechanism of PBP 5 is to obtain a crystal structure in complex with a peptide substrate. Unfortunately, this is very difficult to achieve because the rapid hydrolysis of the acyl−enzyme complex precludes its visualization in a diffraction experiment. An alternative approach is to design analogues of the expected transition state of the reaction (*19*−*21*). Boronyl compounds have proven to be very effective transition-state analogue inhibitors of serine proteases (*22*−*25*) and β-lactamases (*26*−*30*), and the mechanistic similarity of these enzymes with PBPs suggests that a similar approach may also be effective with the PBPs. In addition to providing insight into the mechanism of the enzyme-catalyzed reaction, such compounds can also function as potent inhibitors for the enzyme. Moreover, because boronic acids are resistant to hydrolysis by β-lactamases that inactivate β-lactam antibiotics, they have the potential to be developed into a new class of PBP inhibitors.

Previously, we synthesized a series of potential peptide analogue inhibitors as mimics of the expected transition state of deacylation of PBPs (*31*). The most effective inhibitor against several LMM PBPs, including PBP 5, was a dipeptide boronic acid compound in which a boronyl group replaced the carbonyl of the penultimate D-alanine of the peptide substrate. In this report, we describe the crystal structure at 1.6 Å resolution of PBP 5 in complex with a new boronic acid inhibitor, Boc-γ-D-Glu-L-Lys(Cbz)-D-boroAla, which was designed to resemble the portion of the peptide substrate remaining after acylation and loss of the C-terminal D-alanine (Figure 1). This compound most closely represents an analogue of the deacylation reaction because it has an OH group attached to the boron atom that represents the water molecule attacking the carbonyl of the acyl−enzyme intermediate and does not contain a nitrogen-attached substituent that would correspond to the ultimate D-Ala of the D-Ala-D-Ala substrate. The crystal structure of the complex provides valuable insight into the catalytic mechanism of PBP 5 and suggests that Lys-47 does not act directly in deacylation but rather a hydrogen-bonding network, comprising Lys-213, Ser-110, and a water molecule, is responsible.

EXPERIMENTAL PROCEDURES

Synthesis and Characterization of Inhibitor: Boc-L-Lys-(Cbz)-OFm. Generation of the fluorenylmethyl (Fm) ester was performed as described by Merette et al. (*32*). A solution of 5.7 g of Boc-L-Lys(Cbz)-OH (15 mmol) and 4 g of 9-fluorenylmethylchloroformate (15.5 mmol) in 50 mL dichloromethane (DCM) was cooled to 0 °C, followed by

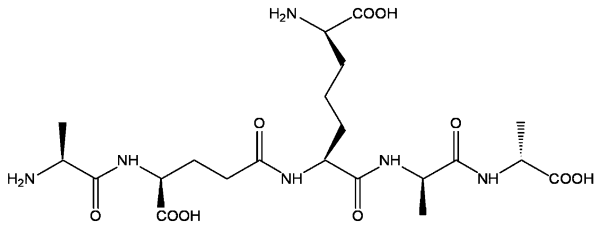

L-Ala-γ-D-Glu-m-DAP-D-Ala-D-Ala

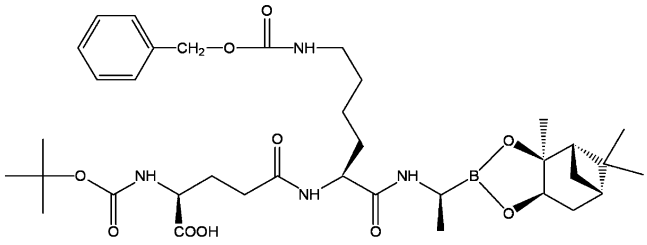

Boc-γ-D-Glu-L-Lyz(Cbz)-D-boroAla-(-)-pinanediol

FIGURE 1: Boronic acid inhibitor used in this study and its similarity to the peptide portion of peptidoglycan. After the loss of the pinanediol group during acylation with PBP 5, the boronic acid inhibitor most closely resembles a tripeptide substrate (γ-D-Glu-*m*-DAP-D-Ala). *m*-DAP = *meso*-diaminopimelic acid, Boc = butyloxycarbonyl, and Cbz = benzyloxycarbonyl.

addition of 3.14 mL of diisopropylethylamine (DIPEA) (18 mmol). After 5 min, 0.2 g (1.65 mmol) of (dimethylamino)-pyridine (DMAP) was added and the reaction mixture was allowed to warm to room temperature. After 2 h at room temperature, the reaction was evaporated to dryness, dissolved in ethyl acetate, and extracted twice each with 2% aqueous citric acid, water, 0.5 N $NaHCO_3$, and finally with water. The ethyl acetate layer was dried over anhydrous $MgSO_4$, evaporated, and dried under vacuum. The oily product was checked by high-pressure liquid chromatography (HPLC) (>98% pure). Liquid chromatography/mass spectrometry (LC/MS): calcd for M^+ (*m*/*z*), 558.3; found, 559.2 ($[M + H]^+$). The yield was calculated after Boc deprotection.

HCl·L-Lys(Cbz)-OFm. Boc-L-Lys(Cbz)-OFm was dissolved in 5 mL of tetrahydrofuran (THF) and cooled to 0 °C, and 10 mL of HCl in glacial acetic acid was added (prepared by flushing 10 mL of ice-cold glacial acetic acid with HCl gas for 15 min). After 90 min, the reaction was evaporated to dryness and the resulting residue was triturated with ether to obtain a solid mass. The solid was dried under vacuum to give a pinkish white crystalline powder (>98% pure, 65% yield). LC/MS: calcd for M^+ (*m*/*z*), 458.4; found, 459.1 ($[M + H]^+$).

Boc-γ-D-Glu(Bzl)-L-Lys(Cbz)-OFm. A solution of 2.53 g of Boc-D-Glu-OBzl (7.5 mmol) and 2.3 mL of *N*-methylmorpholine (NMM) (21 mmol) in 50 mL THF was cooled to −20 °C, followed by addition of 1.0 mL (7.7 mmol) of isobutylchloroformate (IBCF). After 20 min, 3.5 g of L-Lys-(Cbz)-OFm in 20 mL (7 mmol) of dimethylformamide (DMF) was added, the reaction mixture was allowed to warm to room temperature for 2 h and quenched with 1 M $NaHCO_3$, and THF was removed by rotary evaporation. The remaining aqueous suspension was extracted 3 times with equal volumes of ethyl acetate. The combined organic extracts were washed with 1 M HCl and 1 M $NaHCO_3$, dried over anhydrous $MgSO_4$, and evaporated to dryness. The product was recrystallized from ethyl acetate/hexane (>99% pure, 86% yield). LC/MS: calcd for M^+ (*m*/*z*), 777.4; found, 778.1 ($[M + H]^+$).

Boc-γ-D-Glu(Bzl)-L-Lys(Cbz)-OH. To 1.56 g of Boc-γ-D-Glu(Bzl)-L-Lys(Cbz)-OFm (2 mmol), 20 mL of 20% piperidine in DCM was added and the reaction was maintained at room temperature for 90 min. The reaction was evaporated to dryness, dissolved in ethyl acetate, and extracted 4 times with 1 M HCl to remove the Fm-piperidine adduct. The organic layer was dried over anhydrous $MgSO_4$, filtered, rotary evaporated, and dried under vacuum. The white crystalline product was checked by HPLC (>99% pure, 71% yield). LC/MS: calcd for M^+ (*m*/*z*), 599.3; found, 600.3 ($[M + H]^+$).

Boc-γ-D-Glu(Bzl)-L-Lys(Cbz)-D-boroAla-(−)-pinanediol. To a solution of 90 mg of Boc-γ-D-Glu(Bzl)-L-Lys(Cbz)-OH (0.15 mmol) and 50 μL of NMM (0.45 mmol) in 5 mL of DCM at −20 °C was added 21 μL of IBCF (0.17 mmol). After 30 min, 0.056 g of D-boroAla-(−)-pinanediol hydrochloride (0.25 mmol) [prepared as described previously (*31*)] in 2 mL of DMF was added, and the reaction mixture was allowed to warm to room temperature. After 2 h, the reaction mixture was diluted with 25 mL of ethyl acetate and washed successively with 10 mL each of 1 M hydrochloric acid, water, saturated sodium bicarbonate solution, and water. The organic layer was dried over anhydrous $MgSO_4$ and evaporated to dryness. The product was purified by HPLC (52% yield). LC/MS: calcd for M^+ (*m*/*z*), 804.4; found, 805.0 ($[M + H]^+$).

Boc-γ-D-Glu-L-Lys(Cbz)-D-boroAla-(−)-pinanediol. To a solution of Boc-γ-D-Glu(Bzl)-L-Lys(Cbz)-D-boroAla-(−)-pinanediol (50 mg, 0.06 mmol) in 15 mL of 1:1:1 methanol/acetonitrile/water at 0 °C was added 8 mg of K_2CO_3 (0.06 mmol, 1 equiv). After dissolution of K_2CO_3 with stirring, the reaction mixture was kept at 4 °C. Additional 1 equiv aliquots of K_2CO_3 were added to the reaction mixture at 12 and 24 h intervals, and the mixture was incubated for a total of 72 h at 4 °C. Acetonitrile and methanol were evaporated, and the product was purified by HPLC (60% yield). LC/MS: calcd for M^+ (*m*/*z*), 714.4; found, 715.0 ($[M + H]^+$).

Inhibitor Assays. PBP activity assays were performed by quantitation of D-Ala using a D-amino acid oxidase/horseradish peroxidase-coupled enzyme fluorescence assay as described previously (*15*, *33*). Assays were performed with 5 mM Ac_2-L-Lys-D-Ala-D-Ala as the PBP substrate and variable amounts of the inhibitor and were started by addition of PBP. For peptide boronic acid esters, such as the pinandiol ester used in this study, preincubation in the assay buffer releases the free boronic acid from the ester complex for binding to the enzyme (*24*). This substrate concentration is well below the K_m of this substrate for *E. coli* PBP 5 (subsaturating conditions) (*15*). Peptide boronic acids were previously demonstrated to be competitive inhibitors for the PBPs (*31*). Under the conditions of enzyme (PBP) inhibition at subsaturating substrate concentrations ($[S] < K_m$), the following equation will apply:

$$v = v_o/(1 + I/K_I)$$

where v is the observed enzyme-catalyzed rate, v_o is the

uninhibited rate, I is the inhibitor concentration, and K_I is the inhibitor dissociation constant. The K_I value was obtained from the inhibition data by nonlinear regression using SPSS Software (Chicago, IL).

Crystallization of sPBP 5 and Data Collection. Crystals of a soluble construct of wild-type PBP 5 (termed sPBP 5) were grown in the same condition reported previously (*18*). The crystals were then cryoprotected by passage through a solution consisting of mother liquor [8% poly(ethylene glycol) 400 and 100 mM Tris·HCl at pH 8.0] and increasing concentrations of glycerol, in 5% increments, up to a maximum of 25%. Boc-γ-D-Glu-L-Lys(Cbz)-D-boroAla-(−)-pinanediol was then added to this solution to a final concentration of 12.5 mM, and the crystals were allowed to soak for 40 min. Soaking at higher molarities and/or for longer times resulted in a pronounced decrease in the quality of the diffraction. The largest of the crystals was flash-cooled in a gaseous nitrogen stream at 100 K. Data were collected at the SER-CAT ID22 beam line at the Advanced Photon Source (APS), Argonne, IL. A total of 360 images were recorded using a MAR225 CCD detector in 1° oscillations with an exposure time of 1 s per image. The crystal−plate distance was 130 mm. Data were processed with HKL 2000 (*34*).

Structure Determination and Refinement. Wild-type PBP 5 was used as a starting model for refinement. After initial refinement using CNS (*35*), the $|F_{obs}| - |F_{calc}|$ electron-density map was examined for evidence of the inhibitor at the active site. Using the O program (*36*), the boronic acid inhibitor was fitted against both $2|F_{obs}| - |F_{calc}|$ and $|F_{obs}| - |F_{calc}|$ electron-density maps. Subsequent rounds of automated refinement and manual rebuilding were performed with REFMAC (*37*) and O. Library definitions for Boc-γ-D-Glu-L-Lys(Cbz)-D-boroAla were created with the PRODRG2 program (University of Dundee Server) and REFMAC. Where visible, water molecules with reasonable hydrogen-bonding distances were also added to the model. Alternative conformations for several side chains were also modeled (residues 41, 48, 223, 257, 280, and 286). Coordinates and structure factors have been deposited in the Protein Data Bank (PDB ID 1Z6F).

RESULTS

Inhibition Assay. The tripeptide boronic acid compound used in these studies (Boc-γ-D-Glu-L-Lys(Cbz)-D-boroAla) was synthesized and characterized using procedures similar to those described previously (*31*). It was shown to be an effective inhibitor of the D-alanine CPase activity of PBP 5 with a K_I of 13 ± 1 μM (Figure 2). This K_I is much lower than the K_m of 6.4 ± 0.6 mM determined for the corresponding substrate (Boc-γ-D-Glu-L-Lys(Cbz)-D-Ala-D-Ala, unpublished results), indicative of transition-state analogue behavior.

Structure Description. The crystal structure of PBP 5 in complex with Boc-γ-D-Glu-L-Lys(Cbz)-D-boroAla was determined by soaking crystals of wild-type PBP 5 in a solution containing 12.5 mM of the compound for 40 min. The final model has an R factor of 21.3% (R_{free} = 24.0%) with excellent stereochemistry (Table 1) and, at 1.6 Å, is the highest resolution structure of PBP 5 to date. The protein has two domains: domain 1 is comprised of α helices and β strands in a characteristic transpeptidase/penicillin-binding fold found in all PBPs and classes A, C, and D β-lactamases, whereas domain 2 is mostly β-structure. In comparison to the structure of wild-type PBP 5 (*18*), two extra residues, Asn-356 and Phe-357, have been included at the C terminus, which have become visible in the electron-density map because of the improved resolution of the diffraction data.

One important region of the structure appears to occupy two distinct conformations (Figure 3). After refinement, the $|F_o| - |F_c|$ electron-density map contained significant peaks of positive density adjacent to residues 152−154, indicating an alternative route for these residues. This forms part of

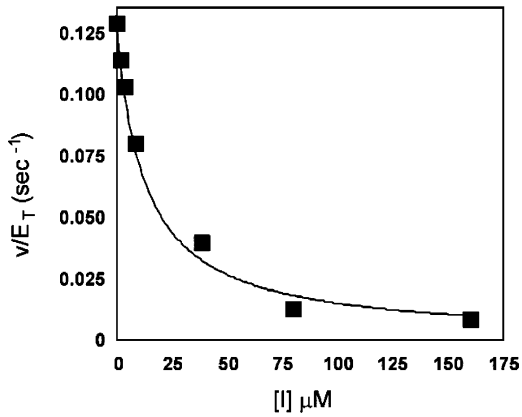

FIGURE 2: PBP 5 DD-CPase activity (y axis) as a function of the boronic acid inhibitor concentration, [I] (x axis). The best fit line produces a K_I value of 13 ± 1 μM.

Table 1: Data Collection and Refinement Statistics of the Structure[a]

data collection	
concentration of soak (mM)	12.5
soak time (min)	40
resolution range (Å)	30.00−1.6 (1.66−1.60)
unit cell (Å)	a = 109.8, b = 50.3, c = 84.3
R_{merge}[b] (%)	6.5 (46.6)
completeness (%)	98.7 (99.9)
average $I/\sigma I$	24.4 (2.4)
number of measurements	231 274
number of unique reflections	52 064
refinement	
reflections used in R_{free} (%)	5
number of non-hydrogen atoms	3192
number of solvent molecules	351
crystallographic R factor (%)	21.5
R_{work} (%)	21.3
R_{free} (%)	24.0
rms deviation from	
ideal stereochemistry	
bond lengths (Å)	0.010
bond angles (deg)	1.36
B factors	
mean B factor (main chain)(Å^2)	18.9
rms deviation in main-chain B factor (Å^2)	0.60
mean B factor (side chains and waters) (Å^2)	23.2
rms deviation in side-chain B factors (Å^2)	1.43
Ramachandran statistics	
residues in most favored region (%)	93.1
residues in additionally allowed regions (%)	6.5
residues in generously allowed regions (%)	0.3
residues in disallowed regions (%)	0.0

[a] Numbers in parentheses are for the outer shell of data. [b] $R_{merge} = \sum_{hkl}\sum_i|I_i(hkl) - \langle I(hkl)\rangle|/\sum_{hkl}\sum_i I_i(hkl)$.

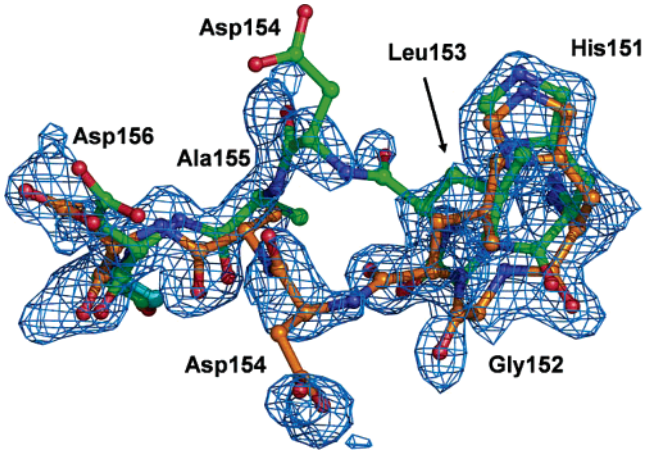

FIGURE 3: Dual conformation of the Ω-like loop in PBP 5. Residues 152−154, inclusive, occupy two conformations as evidenced by positive $|F_o| - |F_c|$ electron density calculated from a model refined in the absence of residues 151−156, shown in blue and contoured at 0.9σ. The chain colored in green occupies the same position as in wild-type PBP 5, whereas the chain colored orange is closer to the active site and its position may result from binding of the boronic acid inhibitor. The figure was made with Pymol (pymol.sourceforge.net).

what has been termed the Ω-like loop in PBP 5, in reference to its spatial overlap with the Ω loop of class A β-lactamases (*12*). In previous structures of PBP 5, general weakness of the electron density in this same region was interpreted as being due to flexibility in the protein chain (*12*, *18*). Interestingly, only one route was traceable in the wild-type structure, and the dual conformations may be the result of the higher resolution of this structure (1.6 Å) compared to that of the wild-type structure (1.85 Å).

Structure of PBP 5 Bound to Boc-γ-D-Glu-L-Lys(Cbz)-D-boroAla. Electron density corresponding to Boc-γ-D-Glu-L-Lys(Cbz)-D-boroAla is clearly visible in the active site of PBP 5 (Figure 4) and is strongest at the boroAla center. Moving away from this center, however, the density gradually weakens toward the branch point of the ligand chain (at L-Lys) and then disappears after the branch point. The electron density of the branch corresponding to the L-lysyl side chain, which terminates at the Cbz group, disappears after the γ carbon of the L-lysine side chain (Figure 4c). The other branch, corresponding to the main chain of the peptide, is visible up to the β carbon of the D-γ-Glu. In each case, peaks of electron density indicate the approximate route of the remainder of each chain but are insufficient to model these regions of the inhibitor with any accuracy. No density corresponding to either of the Boc or Cbz protecting groups is visible. Similarly, there is no electron density corresponding to the pinanediol group of the inhibitor, demonstrating that this protecting group disassociates from the inhibitor upon binding to the enzyme (*24*). Consequently, only those atoms of the inhibitor visible in the electron density have been included in the final model. When these atoms of the inhibitor were refined with full occupancy, the *B* factors of the atoms of the inhibitor closest to Ser-44 were of similar magnitudes with that residue and then gradually increased along the inhibitor chain in accordance with the weakening of the electron density.

The boronic acid inhibitor was designed to be a mimic of the presumed tetrahedral intermediate/transition state for the enzyme-catalyzed deacylation reaction (Scheme 2). The strong electron density between the boron and the γ oxygen of Ser-44, which forms the covalent bond with peptide substrates and β-lactam antibiotics in PBP 5, indicates that a covalent bond is formed between these two atoms. The shape of the electron density around the boron is clearly tetrahedral, consistent with this being a transition-state analogue (Figure 4b).

Scheme 2

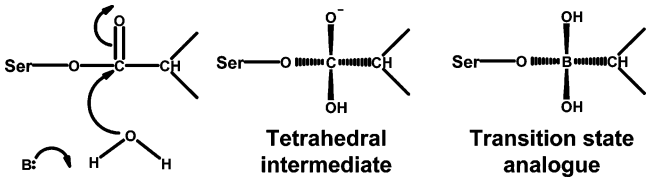

Both of the boronic acid oxygens form hydrogen-bonding interactions within the active site (parts a and c of Figure 4). One oxygen (O2) is within hydrogen-bonding distance of the amide groups of Ser-44 and His-216, which together appear to constitute the oxyanion hole, as well as the carbonyl of His-216. The other oxygen, O3, does not form direct contacts with the enzyme but instead is hydrogen-bonded to two water molecules, W184 and W348. In turn, W184 contacts the main-chain carbonyl of Thr-214 and the γ hydroxyl of Ser-110, and W348 contacts the main-chain amide of His-216 as well the carbonyl group of the γ-D-Glu residue of the inhibitor. Thus, O2 appears to correspond to the oxyanion formed from the carbonyl oxygen of the substrate following attack by a water molecule, while O3 represents the attacking water molecule during hydrolysis of the acyl−enzyme complex (Scheme 2).

Aside from these interactions, there are few other contacts between the inhibitor and PBP 5 (Figure 4c). The main-chain carbonyl group of L-Lys is within hydrogen-bonding distance of both the γ-hydroxyl and main-chain amide of Ser-87 as well as the side-chain amide of Asn-112. Nearby, the main-chain amide of L-Lys is within hydrogen-bonding distance of the carbonyl group of Gly-85. Last, Ser-86 and Leu-153 both may be contributing to hydrophobic packing interactions with the side-chain carbon atoms on the L-Lys substituent.

Of some interest is the protein environment around the boroAla methyl group, which occupies a hydrophobic pocket comprised primarily of Gly-152 and the side chain of Leu-153 and to a lesser degree by Thr-217 and Ala-43. It is noteworthy that Gly-152 and Leu-153 are well-conserved in the class A and C LMM PBPs. Surprisingly, this pocket appears capable of accommodating slightly larger side chains such as valine, which appears contradictory given the specificity of PBPs for a penultimate D-Ala residue in peptide substrates (*38*, *39*), although it is possible that such a cavity is required to accommodate any movement of this group during catalysis. Interestingly, class A β-lactamases also contain a pocket in the equivalent region of the molecule even though β-lactam antibiotics have no substituent occupying this position. For example, in the crystal structure of TEM-1 acylated by penicillin G (*40*), a water molecule lies in approximately the same position as the methyl group of the D-boroAla (not shown). In contrast, such a cavity appears absent in class C β-lactamases: in the crystal structure of AmpC β-lactamase, Tyr-218 occupies this space (*41*).

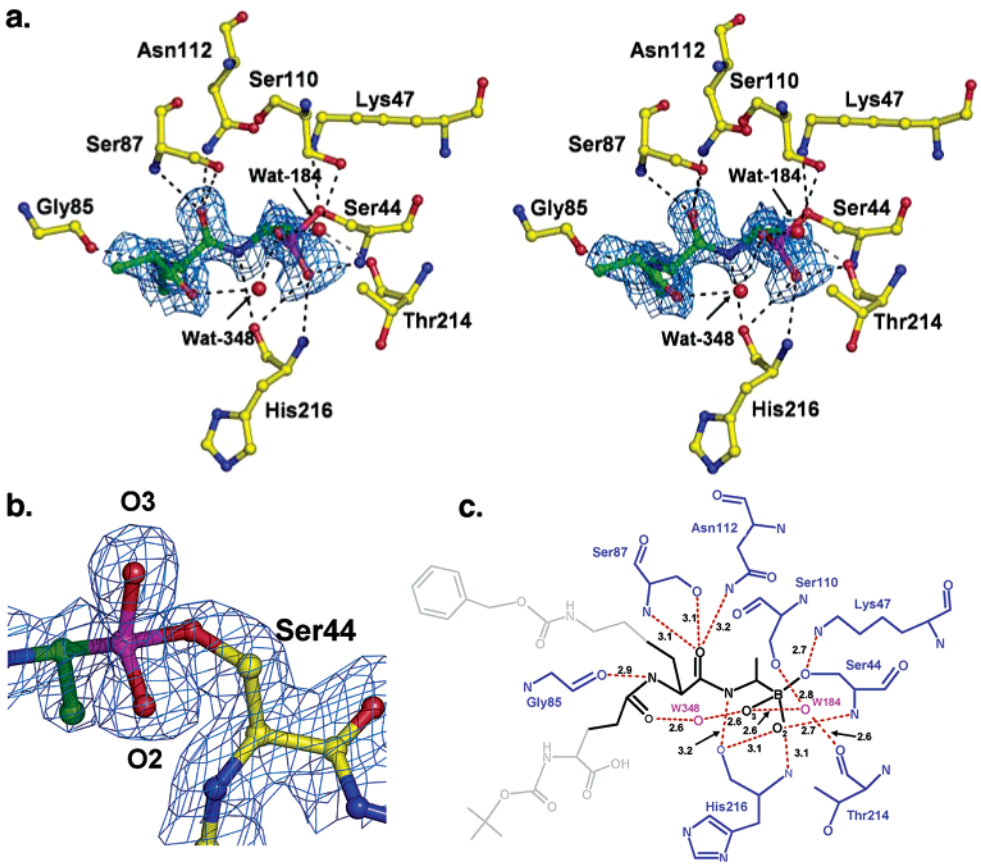

FIGURE 4: Boc-γ-D-Glu-L-Lys(Cbz)-D-boroAla bound in the active site of PBP 5. (a) Stereoview showing the boronic acid inhibitor within the active-site cavity. The electron density is a $|F_o| - |F_c|$ difference map calculated from the final coordinates refined in the absence of the inhibitor. The positive density is shown in blue and is contoured at 1.5σ. The side chains of active-site residues are shown in ball-and-stick form in which carbons are yellow, oxygens are red, and nitrogens are blue. The inhibitor is shown with green bonds, and the boron atom is colored purple. Water molecules are shown as red spheres. Potential hydrogen bonds are shown as dashed lines. (b) Zoom of the region centered on the Ser-44 hydroxyl showing both the covalent bond between Ser-44 and the boron atom and the tetrahedral shape of the density. The images were made with Pymol (pymol.sourceforge.net). (c) Diagram of the contacts made between the boronic acid inhibitor and the active-site residues of PBP 5 (distances in angstroms). Figure created with ISIS Draw (Molecular Design Ltd., U.K.).

The backbone and side chains of the inhibitor each occupy a distinct region on the surface of the protein. The L-lysyl side chain, which is analogous to the *m*-DAP side chain of the peptide substrate, lies within a deep channel parallel to the edge strand of the 5-stranded β sheet of the penicillin-binding domain and residues 82−86. The main-chain branch of the inhibitor comprising the Boc-γ-D-Glu residue lies in a depression on the surface of the protein, lined by residues Gly-85, Ser-86, Ser-87, Leu-88, Phe-90, Gln-109, Gln-195, and Arg-198 (Figure 5). Either (or both) of these regions may comprise the binding site of the natural peptide substrate for EC PBP 5. Interestingly, residues 74−90 exhibited a high degree of disorder in the crystal structure of a mutant of PBP 5 (PBP 5-G105D) that is defective in CPase activity (*12*, *18*, *42*).

Comparison of the Structures of Inhibitor-Bound and Wild-Type PBP 5. The structure of PBP 5 in complex with Boc-γ-D-Glu-L-Lys(Cbz)-D-boroAla superimposes very closely with that of wild-type PBP 5 (*18*), with a (root-mean-square) rms deviation of all Cα distances of 0.6 Å, indicating that the binding of the inhibitor has little effect on the overall structure of the enzyme. However, some interesting differences do occur in and around the active-site region. As noted above, residues 152−154 of this region occupy two conformations (see Figure 3). One of these overlaps with the wild-type structure, but the other is in a new position closer to the active site. In addition, there is a shift in the position of residues 214−223, which comprise a β hairpin between β9 and β10, and in concert, elements adjacent to the β hairpin also move, including the loops prior to β1 and between β10 and α10. Thus, of the five strands that comprise the central β sheet of the penicillin-binding domain in PBP 5, the ends of four strands shift toward the active site in response to the binding of the boronic acid. The biggest shifts in this region occur in residues 217 and 218, which have moved 1.8 and 2 Å, respectively (Cα−Cα distances). This movement appears to be a direct consequence of inhibitor binding because, in the boronic-acid-bound structure, the amide nitrogen of His-216 is within hydrogen-bonding distance of the O2 oxygen of the inhibitor. Furthermore, there is also an interaction between the β hairpin and the Ω-like loop region via a potential hydrogen bond between the side chains of Thr-217 and Asp-154 (Figure 6). In comparison with the native structure, the side chain of Thr-217 has rotated to make this contact, suggesting that this interaction may be important for the stabilization of the oxyanion hole.

Within the active site itself, there is surprisingly little change in the positions of the amino acid residues in the

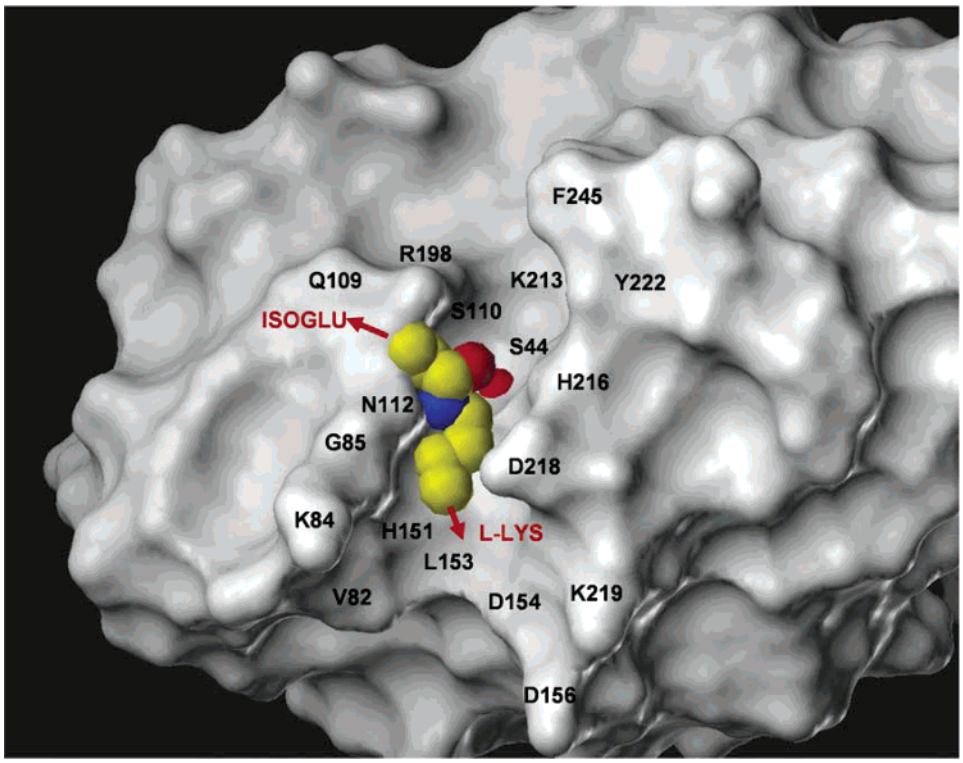

FIGURE 5: Molecular surface of the active-site cavity of PBP 5 showing the boronic acid ligand in CPK form. The positions of some of the amino acid residues that form the binding site are labeled. Red arrows show the approximate directions of the L-Lys side chain and main chain of the inhibitor. The figure was made with Sybyl (Tripos, Inc.).

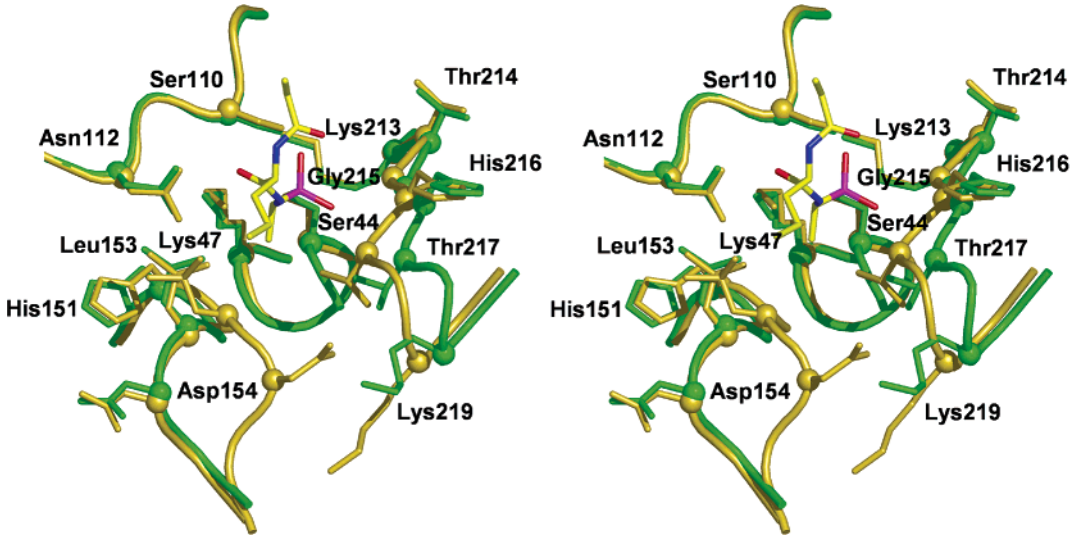

FIGURE 6: Superimposition of the active sites of native and boronic-acid-bound structures of PBP 5. In this stereoview, the structure of native PBP 5 (in green) is compared to that of the complex with the boronic acid inhibitor (gold). The inhibitor is shown in bond form in which carbons are yellow, oxygens are red, nitrogens are blue, and the boron is purple. Important active-site residues are shown in bond form. Note the dual occupancy of the Ω-like loop in the native structure and the shift of the KTG motif toward the active site in the boronic-acid-bound structure. The figure was made with Pymol (pymol.sourceforge.net).

ligand-bound structure compared to the wild-type structure (Figure 6). Much of the hydrogen-bonding network between active-site residues observed in the wild-type structure of PBP 5 (*18*) is retained in the boronic acid complex. Thus, the ϵ-amino group of Lys-213 forms a hydrogen bond with the Oγ of Ser-110 and the main carbonyl oxygens of Ile-106 and Asn-107 (not shown). Ser-44 is within hydrogen-bonding distance of Lys-47, as is Asn-112. Aside from the separation of residues 152−154 into two distinct conformations, as described above, the most significant difference between the native and ligand-bound active sites is the shifts of those residues comprising β9, the edge strand of the central β sheet. Thus, residues Gly-215 to Lys-219, inclusive, are all shifted toward the active site in the boronic-bound structure, with the biggest displacement being in Thr-217.

Comparison with the DD*-Peptidase−Peptide Phosphonate Structure.* The structure of PBP 5 in complex with the boronic acid inhibitor was also compared to that of a DD-peptidase from *Streptomyces* R61 in complex with a peptide

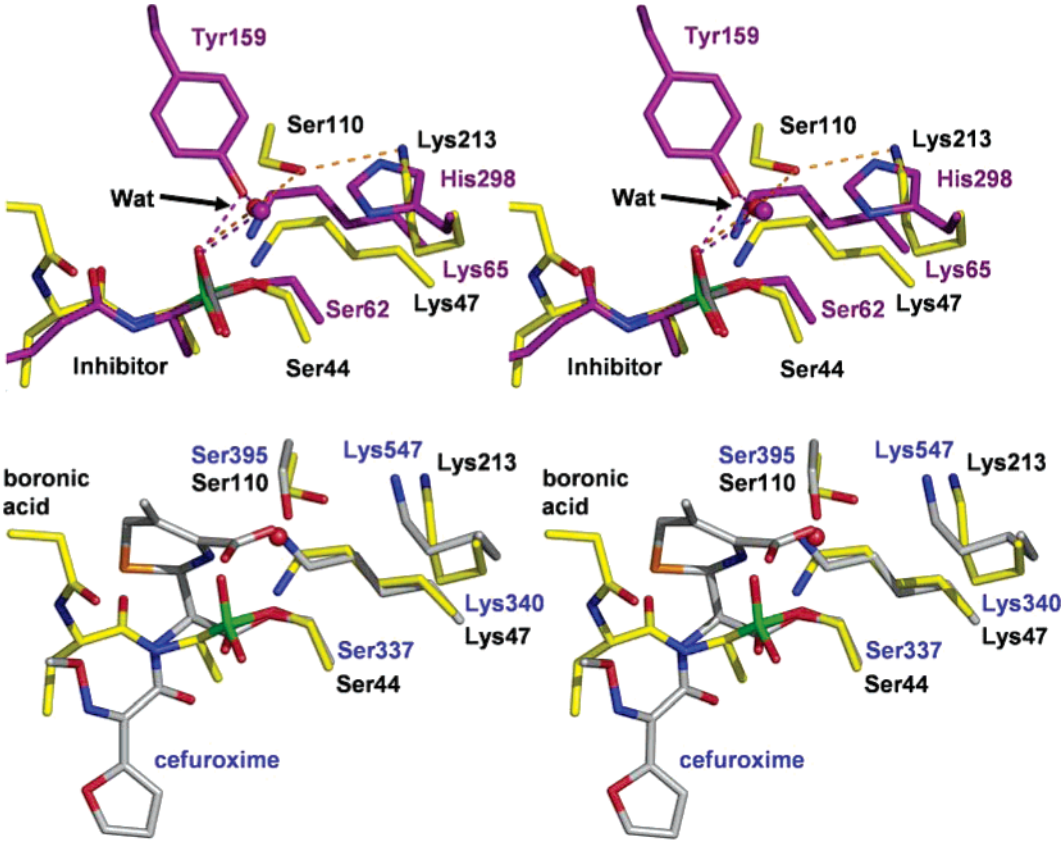

FIGURE 7: Superimposition of the active sites of PBP 5 in complex with the boronic acid inhibitor with two other PBPs. (a) Superimposition with the DD-peptidase from *Streptomyces* R61 in complex with a phosphonate inhibitor (*38*). In this stereoview, the active-site residues of PBP 5 are shown as yellow bonds and those for the DD-peptidase are purple bonds. Oxygens are colored red, nitrogens are blue, the boron is green, and the phosphorus atom is gray. Equivalent residues are labeled black in PBP 5 and purple in the DD-peptidase. Note the similarity in the position of a water molecule adjacent to Tyr-159 in the DD-peptidase and Ser-110 in PBP 5. (b) Superimposition with PBP 2× from *S. pneumoniae* with the same coloring scheme as (a), except that residues of PBP 2× and the antibiotic cefuroxime are colored gray. Residues of PBP 2× are labeled in blue. The figure was made with Pymol (pymol.sourceforge.net).

phosphonate transition-state analogue (*43*). The two enzymes were superimposed using three β strands of the penicillin-binding domain and the SxxK and K(H)TG active-site motifs, and the rms deviation in Cα positions between these common elements was 1.2 Å. Because of the significant difference in structure, the S(Y)xN motif was excluded from the superimposition. The position and geometry of the two amino acid analogues (boroAla and phosphonoAla) within the active site are very similar and overlap closely until the branch point of the boronic acid inhibitor (Figure 7a). The respective serines and lysines of the SxxK motifs also superimpose very closely, but the other active-site residues differ significantly, which may reflect the different substrate specificities of the two enzymes (*15*, *44*, *45*). In PBP 5, Ser-110 and Lys-213 are the equivalents of Tyr-159 and His-298 in the DD-peptidase, respectively. Interestingly, the side-chain hydroxyls of Ser-110 and Tyr-159 are surprisingly close to each other, and each are within hydrogen-bonding distance of a water molecule that occupies a similar position in both active sites. In both cases, the water molecule is also hydrogen-bonded to the same hydroxyl of each inhibitor. A key difference, however, is that Tyr-159 is also hydrogen-bonded directly to O2 (the equivalent atom to O3 in the phosphonate inhibitor), whereas Ser-110 is beyond hydrogen-bonding distance of the O3 atom of the boronic acid inhibitor. Tyr-159 is thought to play the role of general base for deacylation in DD-peptidase (*43*), and the spatial proximity of Ser-110 to Tyr-159 in the superimposition suggests a role for Ser-110 for deacylation in PBP 5 (discussed below).

Comparison with the PBP 2× from Streptomyces pneumoniae. To assess the similarities with a HMM PBP, the structure of the PBP 5−boronic acid complex was also compared to that of PBP 2× from *S. pneumoniae* in complex with the cephalosporin cefuroxime (*11*). With the exception of a serine in place of threonine in the KTG triad, the residues that characterize the conserved motifs of PBPs are the same between the two enzymes. In fact, these residues could be superimposed with a rms deviation between main-chain atoms of 0.58 Å, indicating a close correspondence in the positions of the amino acids in the respective active sites. Despite this, the binding orientation of the boronic acid inhibitor in PBP 5 is strikingly different from that of the antibiotic in PBP 2× (Figure 7b), and its main-chain region approximately bisects the path of the antibiotic. The same is true when also compared to the structure of PBP 2a in complex with antibiotics (*13*) (not shown). Interestingly, O3 of the boronic acid, which is believed to represent the hydrolytic water, essentially overlaps with the β-lactam leaving-group nitrogen of cefuroxime in PBP 2×. If this arrangement was the same in PBP 5 when bound to β-lactam antibiotics, then the hydrolytic water must occupy a different position than O3 of the boronic acid inhibitor. More likely, however, is that PBP 5 binds β lactams differently to the arrangement observed in PBP 2×, and the variety in binding

modes of the thiazolidine (or dihydrothiazine) rings within just the PBP 2a group of acylated structures (*13*) suggests this is indeed the case.

DISCUSSION

The PBPs are a unique enzyme family of bacterial enzymes that catalyze DD-CPase, transpeptidase, and/or endopeptidase reactions required for bacterial cell-wall peptidoglycan biosynthesis. Mechanism-based inhibitors of PBPs are of interest as probes of the essential features of substrate binding and catalytic mechanism in these enzymes, as well as for their potential to be developed into new classes of antibacterial agents. Recently, peptide boronic acids were demonstrated to be effective inhibitors of several PBPs (*31*), and this study presents the first structural description of a PBP−peptide boronic acid complex.

Enzyme−Peptide Interactions. In addition to providing a boronyl group to mimic the transition state of a PBP-catalyzed deacylation reaction, the Boc-γ-D-Glu-L-Lys(Cbz)-D-boroAla inhibitor was designed to incorporate backbone and side-chain elements of the peptide substrate for PBPs. Hence, the crystal structure of the complex also provides clues as to how a peptide substrate might bind in the active site of PBP 5. Other than near the boroAla moiety, there are very few contacts observed between the enzyme and inhibitor. The lack of significant interaction with the distal regions of the inhibitor suggest that many of the *in vivo* enzyme−peptide contacts may be absent in this complex and that the true substrate of PBP 5 may be a larger component of peptidoglycan than is represented in the inhibitor. This may, in turn, explain the relatively low enzymatic activity of PBP 5 against diacetyl-L-Lys-D-Ala-D-Ala-based substrates used to measure CPase activity (*15*, *44*).

The other interesting feature of the inhibitor complex is the orientation of the substrate within the active-site cavity of PBP 5. Electron density corresponding to the carbonyl bond of γ-D-Glu residue is clearly visible, thus distinguishing unequivocally the main-chain branch of the inhibitor from the L-Lys side chain. Moreover, the apparent specificity of the interactions between the L-Lys amide nitrogen and the carbonyl of Gly-85, as well as the carbonyl of γ-D-Glu and a water molecule (W348), suggests that the binding, in terms of overall orientation, is physiologically relevant. The part of the inhibitor that mimics the *m*-DAP side chain, i.e., L-Lys-(Cbz), lies within a deep groove bounded on one side by strand β9, which contains the KT(S)G motif, and on the other side by residues 82−86. This binding mode is broadly the same as that of the glycyl-L-α-aminopimelyl group of the phosphonate inhibitor in the crystal structure of R61 DD-peptidase (*43*). The region of the boronic acid inhibitor that resembles the main chain of the peptide, i.e., the Boc-γ-D-Glu-L-Lys, lies within a depression on the surface of the protein that extends away from the active site (see Figure 5). The existence of a distinct binding region for each branch of the inhibitor, as well as the idea that the enzyme might bind larger molecules than the boronic acid used in this study, suggests that the *in vivo* substrate for PBP 5 might be a cross-linked peptide.

Implications for Catalytic Mechanism. A complete and general description of the catalytic mechanism of PBPs has been elusive. Both acylation and deacylation require withdrawal of a proton from an incipient nucleophile, either from the active-site serine in the acylation reaction or from water or alternative acyl group acceptor in the deacylation reaction. Likewise, both acylation and deacylation require proton donation to the leaving group, either to the C-terminal D-alanine amino group during the acylation reaction or to the active-site serine during the deacylation reaction. On the basis of crystallographic analysis, the pH dependence of enzyme-catalyzed CPase activity, site-directed mutagenesis, and analogy with class A β lactamases, Lys-47 has been proposed as the catalytic base for the acylation reaction in PBP 5 (*12*, *15*, *18*). In this role, Lys-47, in its unprotonated form, withdraws a proton from Ser-44 during nucleophilic attack of the serine hydroxyl on the D-Ala-D-Ala peptide bond. The proximity of Lys-47 to Ser-44 in the crystal structure of PBP 5 in complex with Boc-γ-D-Glu-L-Lys(Cbz)-D-boroAla provides further support for this idea.

A key question remaining, however, is whether Lys-47 also acts as a general base in deacylation or whether another amino acid is involved. The hydroxyl group at O3 of the boronic acid inhibitor, which is analogous to the attacking water molecule for the deacylation reaction, makes no direct interactions with the enzyme; instead, it forms a potential hydrogen bond with a water molecule, W184. This is interesting because a functional group within the active site would be expected to polarize the attacking water molecule to facilitate its attack on the carbonyl carbon of the acyl−enzyme complex. Importantly, this arrangement appears to exclude a direct role for Lys-47 in deacylation because its ϵ-NH_2 group is not close enough (4.2 Å) to O3 to serve as a general base. Although it remains possible that conformational flexibility could move Lys-47 closer to O3 or the initial binding position of the hydrolytic water could be closer to Lys-47, a role for other amino acids in deacylation must be considered.

One residue that might act in the deacylation reaction is Ser-110. Although it is beyond contact range of the O3 hydroxyl of the boronic acid inhibitor in its current position in the crystal structure (see Figure 4), a rotation of its side chain could bring the γ oxygen of Ser-110 to within 2.9 Å of O3. In support of this, evidence of conformational flexibility in the SXN motif has been observed in PBP 5 (unpublished results). Furthermore, such a rotation would increase the degree of overlap between Ser-110 and its tyrosine counterpart in R61 DD-peptidase (see Figure 7a). In the crystal structure of DD-peptidase in complex with a phosphonate inhibitor, Tyr-159 forms a hydrogen bond with O2 of the phosphonate inhibitor (equivalent to O3 of the boronic acid inhibitor); thus, it was proposed that Tyr-159 (in its deprotonated form) acts as the base in deacylation in R61 DD-peptidase by polarizing the hydrolytic water that attacks the carbonyl carbon of the acyl−enzyme complex (*43*). Although a rotation might bring Ser-110 close enough to O3 of the boronic acid inhibitor, it is highly unlikely that Ser-110 in PBP 5 could act as a base because of its high pK_a. This difference, together with the divergent nature of these two CPases, suggests that PBP 5 has a mechanism of deacylation distinct from that of the R61 DD-peptidase.

An alternative mechanism is suggested by the network of hydrogen-bonding interactions linking the hydrolytic water (represented by O3 of the inhibitor), Ser-110, and Lys-213. When Lys-213 acts through this network, it might be the

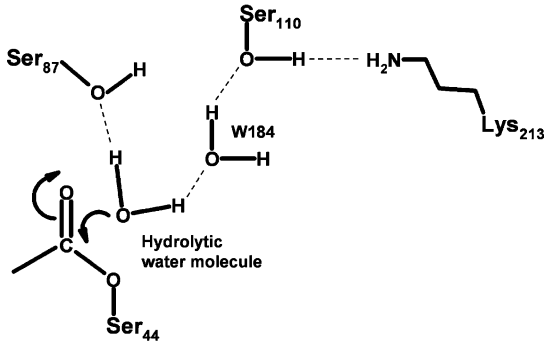

FIGURE 8: Snapshot of the proposed catalytic mechanism for deacylation in PBP 5. Central to this mechanism is a hydrogen-bonding network of amino acid residues and water molecules extending from Lys-213, through Ser-110 and a bridging water molecule (W184), to the hydrolytic water molecule, which serves to orient and polarize the hydrolytic water molecule for attack at the carbonyl carbon of the acyl−enzyme complex. Shown here is the initial step of deacylation that leads to the formation of a tetrahedral intermediate (as represented by the crystal structure of PBP 5 in complex with the boronic acid inhibitor) and includes one plausible arrangement of the hydrogen atoms in the network. Hydrogen bonds are shown as dashed lines. The figure was created with ISIS Draw.

general base for proton extraction from the hydrolytic water molecule. In such a role, its ϵ-amino group must be deprotonated, which might be achieved through hydrogen-bonding interactions with two carbonyls (residues 106 and 107) and a water molecule (W151). Moreover, site-directed mutagenesis demonstrated the importance of Lys-213 in PBP 5, in that substitution to any residue other than arginine resulted in a protein unable to form an acyl−enzyme complex with penicillin G (*46*). However, the K213R mutant showed an identical rate of hydrolysis of the penicilloyl acyl−enzyme complex as the wild-type enzyme (*46*), thus apparently arguing against Lys-213 as a general base, because arginine is unlikely to undergo protonation−deprotonation at physiological pH.

This argument against Lys-213 acting as a general base is predicated on the idea that the mechanisms for deacylation of the peptide substrate and β-lactam antibiotics are the same. However, it is certainly conceivable that the mechanisms are independent, such that Lys-213 is the general base for deacylation for peptidyl−enzyme complexes and a different base is used for the turnover of β-lactam antibiotics. This idea is supported by kinetic data of the K213R enzyme because, although this mutant hydrolyzes the penicilloyl acyl−enzyme complex at a normal rate, it no longer turns over peptide substrates (*46*), suggesting a mechanistic separation of these activities. A similar disparity between the hydrolysis of penicilloyl-PBP and the k_{cat}/K_m for CPase was observed in a S87A mutation of PBP 5 (*18*). A plausible candidate for the general base for acyl−enzyme hydrolysis with β-lactam substrates is the free amino group of the cleaved β-lactam ring, which is tethered in close proximity to the acyl−enzyme intermediate (in contrast to the situation with peptide-based substrates). Such a mechanism has also been proposed previously for the class C β lactamases (*41*, *47*).

The final hypothesis for the mechanism of deacylation in PBP 5 emerging from this study is a subtler one and involves a network of polarizing interactions. In this scenario, Lys-213 promotes deacylation by orienting and polarizing Ser-110, which in turn polarizes the hydrolytic water molecule through the bridging water molecule W184. The polarized hydrolytic water molecule then attacks the electrophilic carbonyl of the acyl−enzyme complex (Figure 8). The proximity of Ser-87 to W184 also suggests a possible contribution of this residue in deacylation of the acyl−enzyme complex. This hypothesis is supported by site-directed mutagenesis experiments in which mutation of Ser-87 to alanine caused a 16-fold decrease of the k_{cat}/K_m constant for CPase activity of PBP 5 (*18*). Irrespective of the precise mechanism of deacylation, evidence from the crystal structure of PBP 5 in complex with the boronic acid inhibitor suggests major roles for Ser-110 and Lys-213 in the deacylation reaction catalyzed by this enzyme.

ACKNOWLEDGMENT

Data were collected at Southeast Regional Collaborative Access Team (SER-CAT) 22-ID beamline at the Advanced Photon Source, Argonne National Laboratory. Supporting institutions may be found at www.ser-cat.org/members.html. Use of the Advanced Photon Source was supported by the U.S. Department of Energy, Office of Science, and Office of Basic Energy Sciences, under contract number W-31-109-Eng-38.

REFERENCES

1. Waxman, D. J., and Strominger, J. L. (1983) Penicillin-binding proteins and the mechanism of action of β-lactam antibiotics, *Annu. Rev. Biochem. 52*, 825−869.
2. Ghuysen, J. M. (1991) Serine β-lactamases and penicillin-binding proteins, *Annu. Rev. Microbiol. 45*, 37−67.
3. Goffin, C., and Ghuysen, J. M. (1998) Multimodular penicillin-binding proteins: An enigmatic family of orthologs and paralogs, *Microbiol. Mol. Biol. Rev. 62*, 1079−1093.
4. Ghuysen, J. M. (1994) Molecular structures of penicillin-binding proteins and β-lactamases, *Trends Microbiol. 2*, 372−380.
5. Holtje, J. V. (1998) Growth of the stress-bearing and shape-maintaining murein sacculus of *Escherichia coli*, *Microbiol. Mol. Biol. Rev. 62*, 181−203.
6. Tipper, D. J., and Strominger, J. L. (1965) Mechanism of action of penicillins: A proposal based on their structural similarity to acyl-D-alanyl-D-alanine, *Proc. Natl. Acad. Sci. U.S.A. 54*, 1133−1141.
7. Schuster, C., Dobrinski, B., and Hakenbeck, R. (1990) Unusual septum formation in *Streptococcus pneumoniae* mutants with an alteration in the D,D-carboxypeptidase penicillin-binding protein 3, *J. Bacteriol. 172*, 6499−6505.
8. Nelson, D. E., and Young, K. D. (2000) Penicillin binding protein 5 affects cell diameter, contour, and morphology of *Escherichia coli*, *J. Bacteriol. 182*, 1714−1721.
9. Stefanova, M. E., Tomberg, J., Olesky, M., Holtje, J. V., Gutheil, W. G., and Nicholas, R. A. (2003) Neisseria gonorrhoeae penicillin-binding protein 3 exhibits exceptionally high carboxypeptidase and β-lactam binding activities, *Biochemistry 42*, 14614−14625.
10. Kelly, J. A., Dideberg, O., Charlier, P., Wery, J. P., Libert, M., Moews, P. C., Knox, J. R., Duez, C., Fraipont, C., Joris, B., et al. (1986) On the origin of bacterial resistance to penicillin: Comparison of a β-lactamase and a penicillin target, *Science 231*, 1429−1431.
11. Gordon, E., Mouz, N., Duee, E., and Dideberg, O. (2000) The crystal structure of the penicillin-binding protein 2× from *Streptococcus pneumoniae* and its acyl−enzyme form: Implication in drug resistance, *J. Mol. Biol. 299*, 477−485.
12. Davies, C., White, S. W., and Nicholas, R. A. (2001) Crystal structure of a deacylation-defective mutant of penicillin-binding protein 5 at 2.3-Å resolution, *J. Biol. Chem. 276*, 616−623.
13. Lim, D., and Strynadka, N. C. (2002) Structural basis for the β lactam resistance of PBP2a from methicillin-resistant *Staphylococcus aureus*, *Nat. Struct. Biol. 9*, 870−876.

14. Fonze, E., Vermeire, M., Nguyen-Disteche, M., Brasseur, R., and Charlier, P. (1999) The crystal structure of a penicilloyl-serine transferase of intermediate penicillin sensitivity. The DD-transpeptidase of streptomyces K15, *J. Biol. Chem. 274*, 21853−21860.
15. Stefanova, M. E., Davies, C., Nicholas, R. A., and Gutheil, W. G. (2002) pH, inhibitor, and substrate specificity studies on *Escherichia coli* penicillin-binding protein 5, *Biochim. Biophys. Acta 1597*, 292−300.
16. Denome, S. A., Elf, P. K., Henderson, T. A., Nelson, D. E., and Young, K. D. (1999) *Escherichia coli* mutants lacking all possible combinations of eight penicillin binding proteins: Viability, characteristics, and implications for peptidoglycan synthesis, *J. Bacteriol. 181*, 3981−3993.
17. Nelson, D. E., and Young, K. D. (2001) Contributions of PBP 5 and DD-carboxypeptidase penicillin binding proteins to maintenance of cell shape in *Escherichia coli*, *J. Bacteriol. 183*, 3055−3064.
18. Nicholas, R. A., Krings, S., Tomberg, J., Nicola, G., and Davies, C. (2003) Crystal structure of wild-type penicillin-binding protein 5 from *E. coli*: Implications for deacylation of the acyl−enzyme complex, *J. Biol. Chem. 278*, 52826−52833.
19. Koehler, K. A., and Lienhard, G. E. (1971) 2-Phenylethaneboronic acid, a possible transition-state analog for chymotrypsin, *Biochemistry 10*, 2477−2483.
20. Schramm, V. L. (1998) Enzymatic transition states and transition state analog design, *Annu. Rev. Biochem. 67*, 693−720.
21. Wolfenden, R. (1999) Conformational aspects of inhibitor design: Enzyme−substrate interactions in the transition state, *Bioorg. Med. Chem. 7*, 647−652.
22. Matteson, D. S., Sadhu, K. M., and Lienhard, G. E. (1981) *R*-1-Acetamido-2-phenylethaneboronic acid. A specific transition-state analog for chymotrypsin, *J. Am. Chem. Soc. 103*, 5241−5242.
23. Kettner, C. A., Bone, R., Agard, D. A., and Bachovchin, W. W. (1988) Kinetic properties of the binding of α-lytic protease to peptide boronic acids, *Biochemistry 27*, 7682−7688.
24. Kettner, C. A., and Shenvi, A. B. (1984) Inhibition of the serine proteases leukocyte elastase, pancreatic elastase, cathepsin G, and chymotrypsin by peptide boronic acids, *J. Biol. Chem. 259*, 15106−15114.
25. Gutheil, W. G., and Bachovchin, W. W. (1993) Separation of L-Pro-DL-boroPro into its component diastereomers and kinetic analysis of their inhibition of dipeptidyl peptidase IV. A new method for the analysis of slow, tight-binding inhibition, *Biochemistry 32*, 8723−8731.
26. Beesley, T., Gascoyne, N., Knott-Hunziker, V., Petursson, S., Waley, S. G., Jaurin, B., and Grundstrom, T. (1983) The inhibition of class C β-lactamases by boronic acids, *Biochem. J. 209*, 229−233.
27. Crompton, I. E., Cuthbert, B. K., Lowe, G., and Waley, S. G. (1988) β-Lactamase inhibitors. The inhibition of serine β-lactamases by specific boronic acids, *Biochem. J. 251*, 453−459.
28. Morandi, F., Caselli, E., Morandi, S., Focia, P. J., Blazquez, J., Shoichet, B. K., and Prati, F. (2003) Nanomolar inhibitors of AmpC β-lactamase, *J. Am. Chem. Soc. 125*, 685−695.
29. Ness, S., Martin, R., Kindler, A. M., Paetzel, M., Gold, M., Jensen, S. E., Jones, J. B., and Strynadka, N. C. (2000) Structure-based design guides the improved efficacy of deacylation transition state analogue inhibitors of TEM-1 β-lactamase, *Biochemistry 39*, 5312−5321.
30. Powers, R. A., Blazquez, J., Weston, G. S., Morosini, M. I., Baquero, F., and Shoichet, B. (1999) The complexed structure and antimicrobial activity of a non-β-lactam inhibitor of AmpC β-lactamase, *Protein Sci. 8*, 2330−2337.
31. Pechenov, A., Stefanova, M. E., Nicholas, R. A., Peddi, S., and Gutheil, W. G. (2003) Potential transition state analogue inhibitors for the penicillin-binding proteins, *Biochemistry 42*, 579−588.
32. Merette, S. A. M., Burd, A. P., and Deadman, J. J. (1999) Synthesis of 9-fluorenylmethyl esters using 9-fluorenylmethylchloroformate, *Tetrahedron Lett. 40*, 753−754.
33. Gutheil, W. G., Stefanova, M. E., and Nicholas, R. A. (2000) Fluorescent coupled enzyme assays for D-alanine: Application to penicillin-binding protein and vancomycin activity assays, *Anal. Biochem. 287*, 196−202.
34. Otwinowski, Z., and Minor, W. (1997) Processing of X-ray diffraction data collected in oscillation mode, *Methods Enzymol. 276*, 307−326.
35. Brunger, A. T., Adams, P. D., Clore, G. M., DeLano, W. L., Gros, P., Grosse-Kunstleve, R. W., Jiang, J. S., Kuszewski, J., Nilges, M., Pannu, N. S., Read, R. J., Rice, L. M., Simonson, T., and Warren, G. L. (1998) Crystallography and NMR system: A new software suite for macromolecular structure determination, *Acta Crystallogr., Sect. D 54*, 905−921.
36. Jones, T. A., Zou, J.-Y., Cowan, S. W., and Kjeldgaard, M. (1991) Improved methods for building protein structures in electron-density maps and the location of errors in these models, *Acta Crystallogr., Sect. A 47*, 110−119.
37. Murshudov, G. N., Vagin, A. A., and Dodson, E. J. (1997) Refinement of macromolecular structures by the maximum-likelihood method, *Acta Crystallogr., Sect. D 53*, 240−255.
38. Georgopapadakou, N., and Sykes, R. B. (1983) Bacterial enzymes interacting with β-lactam antibiotics, *Handb. Exp. Pharmacol. 67*, 1−77.
39. Ghuysen, J. M., Frere, J. M., Leyh-Bouille, M., Coyette, J., Dusart, J., and Nguyen-Disteche, M. (1979) Use of model enzymes in the determination of the mode of action of penicillins and δ 3-cephalosporins, *Annu. Rev. Biochem. 48*, 73−101.
40. Strynadka, N. C., Adachi, H., Jensen, S. E., Johns, K., Sielecki, A., Betzel, C., Sutoh, K., and James, M. N. (1992) Molecular structure of the acyl−enzyme intermediate in β-lactam hydrolysis at 1.7 Å resolution, *Nature 359*, 700−705.
41. Patera, A., Blaszczak, L., and Shoichet, B. (2000) Crystal structures of substrate and inhibitor complexes with AmpC β-lactamase: Possible implications for substrate-assisted catalysis, *J. Am. Chem. Soc. 122*, 10504−10512.
42. Nicholas, R. A., and Strominger, J. L. (1988) Site-directed mutants of a soluble form of penicillin-binding protein 5 from *Escherichia coli* and their catalytic properties, *J. Biol. Chem. 263*, 2034−2040.
43. Silvaggi, N. R., Anderson, J. W., Brinsmade, S. R., Pratt, R. F., and Kelly, J. A. (2003) The crystal structure of phosphonate-inhibited D-Ala-D-Ala peptidase reveals an analogue of a tetrahedral transition state, *Biochemistry 42*, 1199−1208.
44. Anderson, J. W., Adediran, S. A., Charlier, P., Nguyen-Disteche, M., Frere, J. M., Nicholas, R. A., and Pratt, R. F. (2003) On the substrate specificity of bacterial DD-peptidases: Evidence from two series of peptidoglycan-mimetic peptides, *Biochem. J. 373*, 949−955.
45. Anderson, J. W., and Pratt, J. M. (2000) Dipeptide binding to the extended active site of the *Streptomyces* R61 D-alanyl-D-alanine-peptidase: The path to a specific substrate, *Biochemistry 39*, 12200−12209.
46. Malhotra, K. T., and Nicholas, R. A. (1992) Substitution of lysine 213 with arginine in penicillin-binding protein 5 of *Escherichia coli* abolishes D-alanine carboxypeptidase activity without affecting penicillin binding, *J. Biol. Chem. 267*, 11386−11391.
47. Bulychev, A., Massova, I., Miyashita, K., and Mobashery, S. (1997) Nuances of mechanisms and their implications for evolution of the versatile β-lactamase activity: From biosynthetic enzymes to drug resistance factors, *J. Am. Chem. Soc. 119*, 7619−7625.

BI0473004